ISSN 0915-633X

NATIONAL INSTITUTE FOR FUSION SCIENCE

Effect of Ambient Gas on Three-Dimensional Breakup in Coronet Formation Process

Takashi Yabe and Yan Zhang

(Received - Feb. 16, 1998)

NIFS-539 Feb. 1998

RESEARCH REPORT
NIFS Series

NAGOYA, JAPAN

Effect of Ambient Gas on Three-Dimensional Breakup in Coronet Formation Process

Takashi Yabe, Yan Zhang

Department of Energy Sciences, Tokyo Institute of Technology
4259 Nagatsuta, Midoriku, Yokohama 226, Japan

Abstract

We have succeeded for the first time to simulate the three-dimensional breakup of thin film in coronet formation process. Surprisingly, the wavelength of the irregularity along the rim of coronet sensitively depends on the density of ambient gas and linearly increases with gas density although its density is negligibly small. Therefore the Rayleigh-Taylor instability alone can not explain the phenomena ; nevertheless the deceleration may be responsible for the breakup. The simulation suggests that the breakup is due to competing between Kelvin-Helmholtz instability and Rayleigh-Taylor instability. The maximum wave number is reached when the breakup driven by R-T overcomes the swelling-up of the rim owing to K-H instability and is inversely proportional to gas density.

Keywords : Milk Crown, Simulation, Three-Dimension, Ambient Gas, Surface Capture

Since the pioneering work by Worthington*(1)*, the coronet or the so-called milk-crown has been investigated mostly by experiments that already revealed many interesting features and physics included*(2,3)*. In contrast, simulation of the coronet has long been a dream in the field of computational physics because it can not only demonstrate the power of the scheme but also can investigate the physics of the coronet formation by choosing a situation which can be hardly realized by experiments. Several interface capturing schemes have been proposed to attack this problem. Although the present-day technique is already close to this goal, nobody reported the three-dimensional coronet formation before except for a preliminary three-dimensional work*(4)*, and several two-dimensional works pioneered by Harlow & Shannon*(5)*, in which instability and therefore breakup of rim leading to the coronet were not simulated. This is because the coronet is not merely a consequence of a free surface problem but we must treat ambient gas as well. This requires a special treatment at the complex boundary of the coronet where density ρ changes by 1000 times. In solving pressure p, it is quite a difficult task to guarantee the continuity of force $(\nabla p)/\rho$ across the complex interface having very large density ratio, otherwise quite a large acceleration can occur because of the change of denominator from 1 to 0.001 g/cm^3 across the interface.

Recently we have developed a new computational algorithm CIP*(6-8)* (cubic-interpolated propagation) which can treat the interface of liquid and gas with almost one grid even in the fixed Cartesian grid system. The VOF*(9)*(volume of fluid) and LSF*(10)* (level set function) may have a similar capability. The CIP has further advantage that it can solve all the phases of matter together from solid through liquid to gas because it can treat very large density change keeping the continuity of $(\nabla p)/\rho$ at the interface without any special boundary condition. These advantages of the CIP have been demonstrated in the simulation of the melting and evaporation dynamics of metal irradiated by laser light*(8)*. This capability is essential for the application to the instability during the dynamics of coronet formation.

Figure 1 shows an iso-surface contour of density in which 100 × 100(horizontal) × 34(vertical) fixed, equally spaced Cartesian grids are used with 0.1 cm grid spacing. A thin water film of 0.4 cm thick is placed on a solid plate and a water drop of 0.8 cm radius impacts from the top at a speed of 50 cm/sec. We solved gas as well as water and the density ratio at the interface is almost 1000 as already mentioned. As shown in Fig.1 at t=52 and 88 ms, the irregular ring, which we call "ornament" of the coronet, appears at first and then laminar belt develops below the ornament later on at 152 and 240 ms in Fig.1.

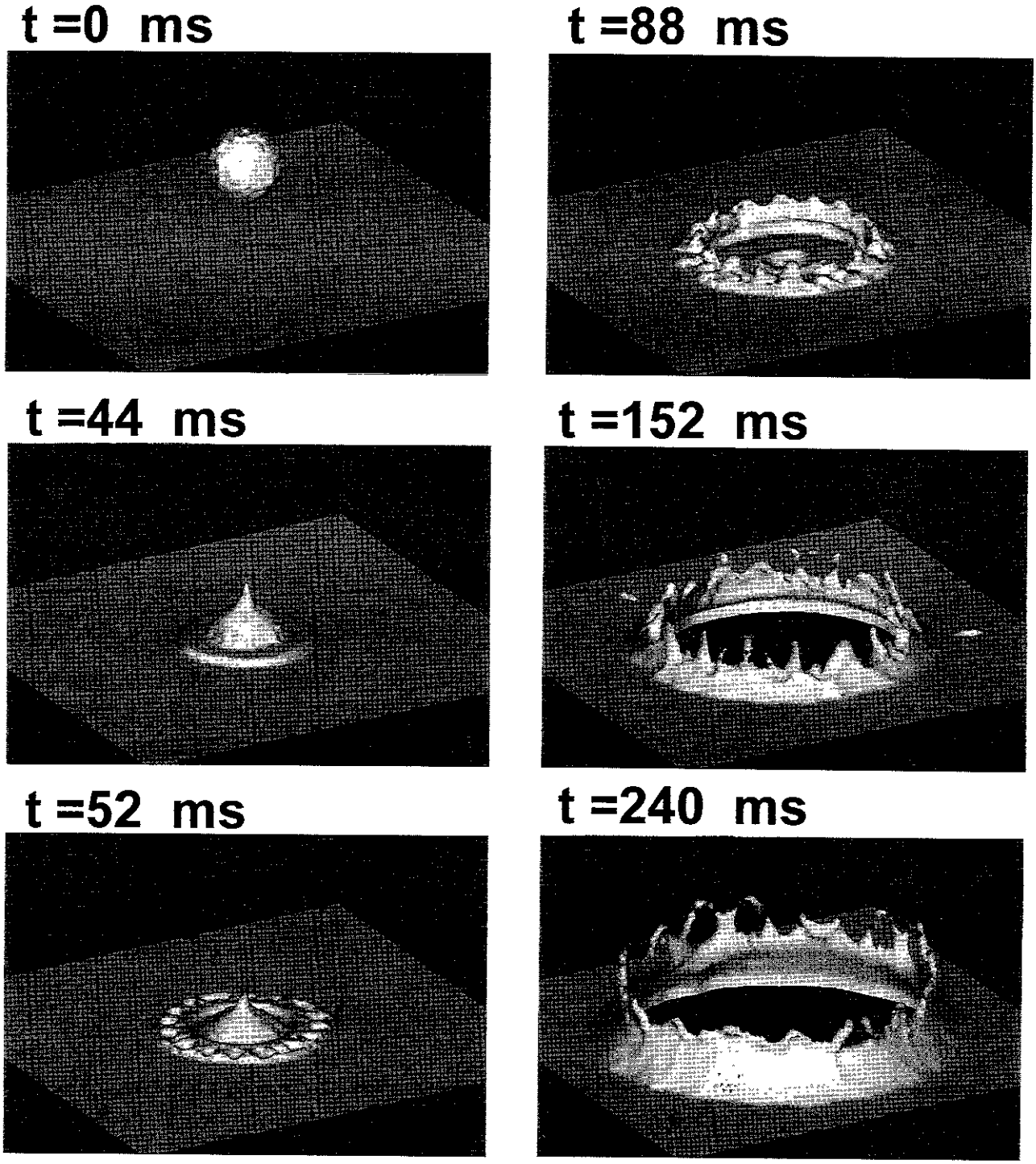

Fig.1 : Water surface plot in the coronet formation process. 100×100×34 Cartesian grid is used. After impact until t=44 ms, flat ring of thin film like a "washer" appears on the original film. At t=52 and 88 ms, the irregular ring, which we call "ornament" of the coronet, appears at first and then laminar belt develops below the ornament later on at 152 and 240 ms

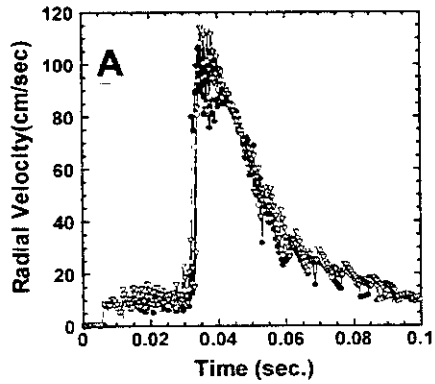

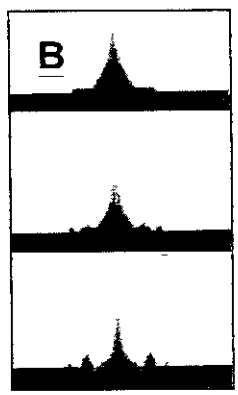

Fig.2 : **(A)** Time evolution of radial velocity, where closed circles, open circles and triangles show the velocity for the case of ρ_{gas}=0.001, 0.005 and 0.01, respectively. At the time of impact t=32 ms, large acceleration occurs and then deceleration follows after 44 ms until 60 ms In the latter phase, the Rayleigh-Taylor instability can grow at the rim caused by a snow plough and Kelvin-Helmholtz instability. **(B)** Cross-sectional view of the water at 48, 52 and 60 ms from the top.

The time evolution of the radial expansion velocity of the coronet can shed light on the formation mechanism of these structures. In the simulation of Fig.2 we performed two-dimensional axisymmetric simulation to avoid the influence of the instability on the main flow driving instability. Upon impact of the drop onto the liquid surface, liquid film is pushed radially outwards like a snow plough. The radial motion is initially accelerated by the high pressure of impact and then decelerated as shown in Fig.2A. After impact until t=44 ms, flat ring of thin film like a "washer" appears on the original film as shown in Fig.1 because of raking up by a snow plough. The outer radius of the washer is 1.5 cm at t=44 ms and inner radius in contact with the drop is 0.8 cm, between these radii the washer thickness is extremely uniform. Around t=44 ms, deceleration starts and then outer leading edge of the washer moves apart from the main ring as shown in the density contour in Fig.2, while the main ring gradually shrinking to the same radius and giving rise to a large hump which grows into a circular rim and eventually leads to the coronet. This rim becomes unstable at the deceleration phase.

If the breakup of the rim had been caused by the effect of finite-sized rectangular grids, its effect would have already appeared at this early stage(t<44ms). On the contrary, the breakup abruptly occurs just at the time when deceleration starts and thus some instability may take place. Furthermore, as it will be shown later, the wavelength of the irregularity along the rim changes depending on the density of ambient gas. This proves that the breakup observed here is not an artifact of finite grid size although it might have provided seeds of the instability.

From Fig.2, we can estimate the deceleration of the motion to be a=2.3 × 10^3cm/sec^2 and from typical wavelength 0.67 cm (k=10) of the irregularity along the rim during deceleration we get the growth rate of $\gamma_{RT}=(ak)^{1/2}$=151 sec^{-1} for the R-T (Rayleigh-Taylor) instability. This growth rate seems to be sufficient to account for the evolution of the irregularity because of $\gamma \triangle t$=3.93 during the deceleration time $\triangle t$=26 ms. At t=60 ms, the deceleration is largely reduced and from this time on, because of the lack of the instability, laminar belt of the coronet begins to develop just below the ornament. Thus the well-known double structure consisting of the ornament on top of the laminar belt is formed as observed in typical experiment of the coronet *(1)*.

The above observation looks reasonable. Since the computer capability is limited, we can not check the validity of the theory by largely changing the parameters. The easiest and most interesting way to alter the situation is to change the gas density ρ_{gas}. Although the denser gas seems to be unrealistic, it may help to check the physics in a situation which can be realized only by computer simulation. Since the gas density is 1000 times less than water, it may not contribute to the evolution of the coronet. Surprisingly , however, it sensitively changes the evolution as shown in this paper.

Figure 3 shows the density contour of water sliced horizontally in the middle of the rim. Interestingly, unstable wavelength becomes longer when gas density is increased, and finally at the gas density of 0.01 g/cm^3 the mode number is reduced

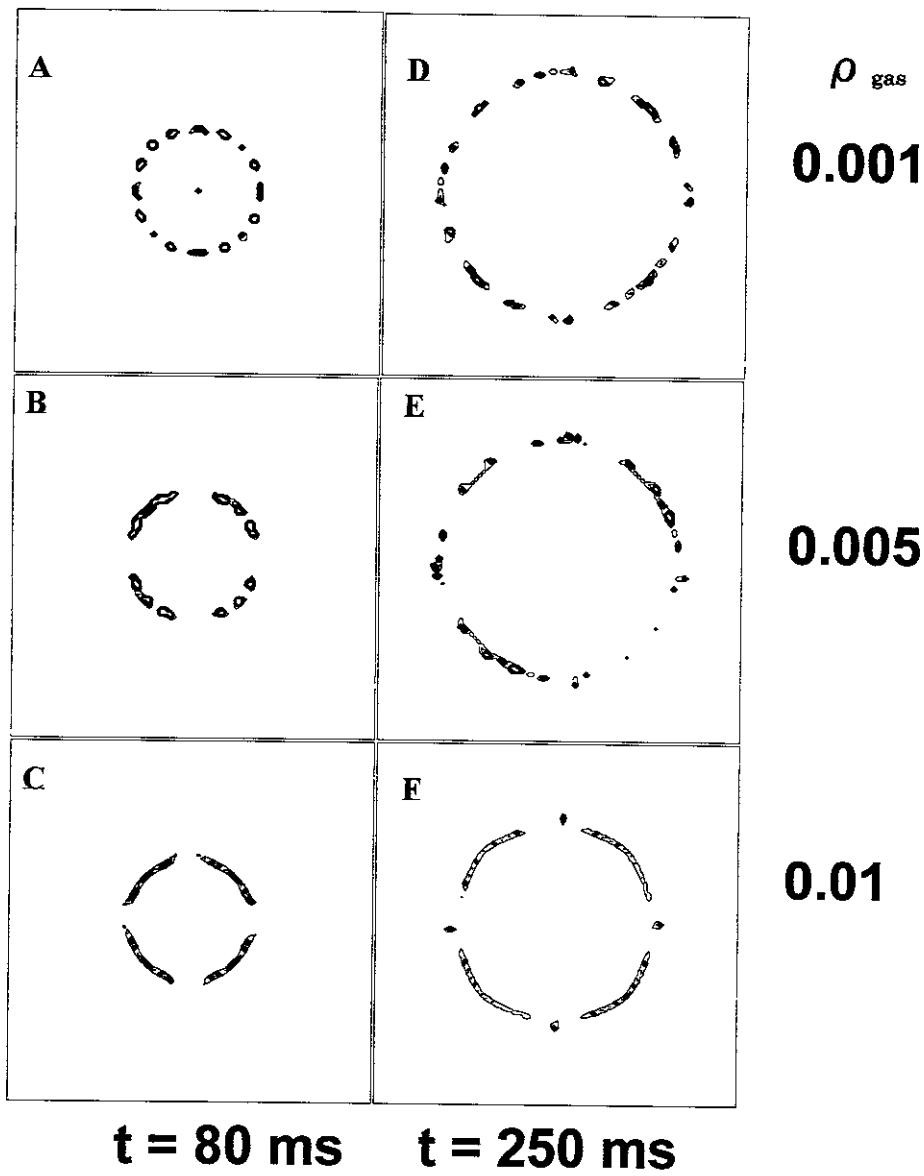

Fig.3 : Density contour of the rim for the gas density of (**A** and **D**) 0.001, (**B** and **E**) 0.005 and (**C** and **F**) 0.01 g/cm^3. Left three figures (**A,B,C**) show the contours at 80 ms and right three figures (**D,E,F**) show those at 250 ms.

to 4. Figures 3A-C show the density contour at t=80ms and Figs.3D-F show that at t=250ms. As shown in the figure, different nature of the breakup is already seen at this early stage of t=80ms when the deceleration has just stopped.

We have also displayed the time evolution of radial velocity for these cases in Fig.2, where closed circles, open circles and triangles show the velocity for the case of ρ_{gas} =0.001, 0.005 and 0.01, respectively. This time evolution seems to be similar for any density of gas and the deceleration time is slightly longer for denser gas. If this deceleration had caused the breakup, then denser gas and hence long deceleration time would have made the irregularity be slightly larger. This contradicts with the observation in Fig.3. Although the gas density comes into the growth rate as the Attwood number = $[(\rho_{water}-\rho_{gas})/(\rho_{water}+\rho_{gas})]^{1/2}$, it is too small already to change the number even for denser gas of 0.01 g/cm^3 compared with the water density ρ_{water} =1g/cm^3.

If the instability is caused by the K-H (Kelvin-

Helmholtz) instability, the growth rate *(11)* is $\gamma_{KH} = k|U|(\rho_{water}\rho_{gas})^{1/2}/(\rho_{water}+\rho_{gas})$, where U is the relative velocity between gas and water, and can be affected by the ambient gas density by a factor of 3 for 10 times difference of density. However, the growth rate is larger for denser gas and contradicts with the simulation result.

Here we propose one possible explanation to this result. The K-H instability drives the swelling-up of the rim to the vertical direction instead of breakup, while the R-T instability acts as to breakup the thin film of the rim along the azimuthal direction and thus causes the "ornament". If $\gamma_{KH} > \gamma_{RT}$, then the breakup becomes slower than swelling-up and therefore the coronet will not be formed. Thus the criterion for the breakup should be

$$\gamma_{RT} \geq \gamma_{KH} \quad \Rightarrow \quad \frac{k\rho_{water}\rho_{gas}}{(\rho_{water}-\rho_{gas})(\rho_{water}+\rho_{gas})} \leq \frac{a}{U^2} \qquad (1)$$

If this relation is correct, the maximum wave number is inversely proportional to gas density. In fact, the wavelength of the ornament is approximately proportional to gas density as shown in Fig.4, where circles and squares represent the wavelength at 80 and 250 ms observed in Fig.3, respectively. Two same symbols at the same density, for example two squares at ρ_{gas}=0.01g/cm^3, mean ambiguity of the measured wavelength. This justifies the relation (1) because a and U are similar regardless of gas density.

In the simulation, we have included the kinematic viscosity for water and air to be 0.01 and 0.15 cm^2/sec, respectively. Since the viscosity effect appears in a form of kinematic viscosity in the R-T and K-H instability, the effect of the ambient density will not explicitly appear in the result. Although we have not included the surface tension here, it may not drive the instability in the thin film of the rim but rather it will contribute to the droplet formation after the instability fully develops.

In summary, we have succeeded for the first time to simulate the three-dimensional formation process of the coronet. The wavelength of the irregularity along the rim depends on the density of ambient gas and linearly increases with the density. This is due to competing between swelling-up of the rim owing to K-H instability and breakup owing to R-T instability. The present simulation has added important knowledge to the coronet formation physics by choosing the situation which would be hardly realized by the experiments.

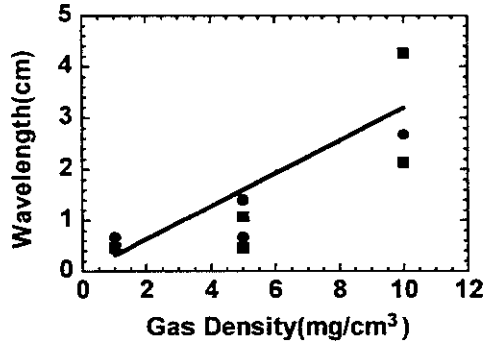

Fig.4 : Circles and squares represent the wavelength at 80 and 250 ms observed in Fig.3, respectively. Two same symbols at the same density, for example two squares at ρ_{gas}=0.01, mean ambiguity of the measured wavelength.

This work was carried out under the collaborating research program at the National Institute for Fusion Science of Japan.

REFERENCES AND NOTES

1. A.M.Worthington, A Study of Splashes. London:Longman & Green (1908); reprinted 1963, New York:Macmillan.
2. H.E.Edgerton and J.R.Killian, Moments of Vision. Boston:MIT Press. (1987).
3. P.V.Hobbs and T.Osheroff , *Science* **158**, 1184(1967)
4. A.Prosperetti and H.N.Oguz, *Annu. Rev. Fluid Mech.* **25**,577 (1993).
5. F.H.Harlow and J.P.Shannon , *J.Appl.Phys.* **38**,3855 (1967).
6. H.Takewaki, A.Nishiguchi, T.Yabe, *J. Comput. Phys.* **61**,261 (1985).
7. T.Yabe and T.Aoki,*Comput.Phys.Commun.* **66** ,219 (1991).
8. T.Yabe and F.Xiao, *Nucl.Eng. & Design.* **155**, 45(1995).
9. C.W.Hirt and B.D.Nichols , *J.Comput.Phys.* **39**,201 (1981).
10. S.Osher and J.A.Sethian , *J.Comput.Phys.* **79**,12 (1988)
11. S.Chandrasekhar , Hydrodynamic and Hydromagnetic Stability (Dover Pub., New York, 1961).

Recent Issues of NIFS Series

NIFS-502 V Vdovin, T Watari and A Fukuyama,
An Option of ICRF Ion Heating Scenario in Large Helical Device, July 1997

NIFS-503 E Segre and S Kida,
Late States of Incompressible 2D Decaying Vorticity Fields, Aug 1997

NIFS-504 S Fujiwara and T Sato,
Molecular Dynamics Simulation of Structural Formation of Short Polymer Chains, Aug 1997

NIFS-505 S Bazdenkov and T Sato
Low-Dimensional Model of Resistive Interchange Convection in Magnetized Plasmas, Sep 1997

NIFS-506 H Kitauchi and S Kida,
Intensification of Magnetic Field by Concentrate-and-Stretch of Magnetic Flux Lines, Sep 1997

NIFS-507 R.L Dewar,
Reduced form of MHD Lagrangian for Ballooning Modes, Sep. 1997

NIFS-508 Y -N Nejoh,
Dynamics of the Dust Charging on Electrostatic Waves in a Dusty Plasma with Trapped Electrons, Sep.1997

NIFS-509 E Matsunaga, T Yabe and M. Tajima,
Baroclinic Vortex Generation by a Comet Shoemaker-Levy 9 Impact, Sep 1997

NIFS-510 C C Hegna and N. Nakajima,
On the Stability of Mercier and Ballooning Modes in Stellarator Configurations; Oct. 1997

NIFS-511 K Ohto and T Hatori,
Rotation and Oscillation of Nonlinear Dipole Vortex in the Drift-Unstable Plasma; Oct. 1997

NIFS-512 J. Uramoto,
Clear Detection of Negative Pionlike Particles from H_2 Gas Discharge in Magnetic Field; Oct 1997

NIFS-513 T Shimozuma, M Sato, Y. Takita, S. Ito, S Kubo, H Idei, K. Ohkubo, T Watari, T S Chu, K. Felch, P. Cahalan and C.M. Loring, Jr,
The First Preliminary Experiments on an 84 GHz Gyrotron with a Single-Stage Depressed Collector, Oct 1997

NIFS-514 T Shimozuma, S Morimoto, M Sato, Y. Takita, S Ito, S Kubo, H Idei, K Ohkubo and T. Watari,
A Forced Gas-Cooled Single-Disk Window Using Silicon Nitride Composite for High Power CW Millimeter Waves, Oct. 1997

NIFS-515 K. Akaishi,
On the Solution of the Outgassing Equation for the Pump-down of an Unbaked Vacuum System, Oct. 1997

NIFS-516 *Papers Presented at the 6th H-mode Workshop (Seeon, Germany)*; Oct. 1997

NIFS-517 John L. Johnson,
The Quest for Fusion Energy; Oct. 1997

NIFS-518 J. Chen, N Nakajima and M. Okamoto,
Shift-and-Inverse Lanczos Algorithm for Ideal MHD Stability Analysis, Nov 1997

NIFS-519 M Yokoyama, N Nakajima and M. Okamoto,
Nonlinear Incompressible Poloidal Viscosity in L=2 Heliotron and Quasi-Symmetric Stellarators, Nov 1997

NIFS-520 S. Kida and H. Miura,
Identificaiton and Analysis of Vortical Structures; Nov. 1997

NIFS-521 K. Ida, S. Nishimura, T. Minami, K. Tanaka, S. Okamura, M. Osakabe, H. Idei, S Kubo, C. Takahashi and K. Matsuoka,
High Ion Temperature Mode in CHS Heliotron/torsatron Plasmas; Nov. 1997

NIFS-522 M. Yokoyama, N. Nakajima and M. Okamoto,
Realization and Classification of Symmetric Stellarator Configurations through Plasma Boundary Modulations; Dec. 1997

NIFS-523 H. Kitauchi,
Topological Structure of Magnetic Flux Lines Generated by Thermal Convection in a Rotating Spherical Shell; Dec. 1997

NIFS-524 T. Ohkawa,
Tunneling Electron Trap; Dec. 1997

NIFS-525 K. Itoh, S.-I. Itoh, M. Yagi, A. Fukuyama,
Solitary Radial Electric Field Structure in Tokamak Plasmas; Dec. 1997

NIFS-526 Andrey N. Lyakhov,
Alfven Instabilities in FRC Plasma, Dec. 1997

NIFS-527 J. Uramoto,
Net Current Increment of negative Muonlike Particle Produced by the Electron and Positive Ion Bunch-method; Dec. 1997

NIFS-528 Andrey N. Lyakhov,
Comments on Electrostastic Drift Instabilities in Field Reversed Configuraiton; Dec. 1997

NIFS-529 J. Uramoto,
Pair Creation of Negative and Positive Pionlike (Muonlike) Particle by Interaction between an Electron Bunch and a Positive Ion Bunch; Dec 1997

NIFS-530 J. Uramoto,
Measuring Method of Decay Time of Negative Muonlike Particle by Beam Collector Applied RF Bias Voltage; Dec. 1997

NIFS-531 J. Uramoto,
Confirmation Method for Metal Plate Penetration of Low Energy Negative Pionlike or Muonlike Particle Beam under Positive Ions; Dec. 1997

NIFS-532 J. Uramoto,
Pair Creations of Negative and Positive Pionlike (Muonlike) Particle or K Mesonlike (Muonlike) Particle in H2 or D2 Gas Discharge in Magnetic Field; Dec. 1997

NIFS-533 S. Kawata, C. Boonmee, T Teramoto, L. Drska, J. Limpouch, R. Liska, M. Sinor,
Computer-Assisted Particle-in-Cell Code Development; Dec. 1997

NIFS-534 Y. Matsukawa, T. Suda, S. Ohnuki and C. Namba,
Microstructure and Mechanical Property of Neutron Irradiated TiNi Shape Memory Alloy; Jan. 1998

NIFS-535 A. Fujisawa, H. Iguchi, H. Idei, S. Kubo, K. Matsuoka, S. Okamura, K. Tanaka, T. Minami, S. Ohdachi, S. Morita, H. Zushi, S Lee, M. Osakabe, R. Akiyama, Y. Yoshimura, K. Toi, H. Sanuki, K. Itoh, A. Shimizu, S. Takagi, A Ejiri, C. Takahashi, M. Kojima, S Hidekuma, K. Ida, S. Nishimura, N. Inoue, R. Sakamoto, S -I. Itoh, Y. Hamada, M. Fujiwara,
Discovery of Electric Pulsation in a Toroidal Helical Plasma; Jan. 1998

NIFS-536 Lj.R. Hadzievski, M.M. Skoric, M. Kono and T. Sato,
Simulation of Weak and Strong Langmuir Collapse Regimes; Jan. 1998

NIFS-537 H. Sugama, W. Horton,
Nonlinear Electromagnetic Gyrokinetic Equation for Plasmas with Large Mean Flows; Feb 1998

NIFS-538 H. Iguchi, T.P. Crowley, A. Fujisawa, S. Lee, K. Tanaka, T. Minami, S. Nishimura, K. Ida, R. Akiyama, Y. Hamada, H., Idei. M. Isobe, M. Kojima, S. Kubo, S. Morita, S. Ohdachi, S. Okamura, M. Osakabe, K. Matsuoka, C. Takahashi and K. Toi,
Space Potential Fluctuations during MHD Activities in the Compact Helical System (CHS); Feb. 1998

NIFS-539 Takashi Yabe and Yan Zhang,
Effect of Ambient Gas on Three-Dimensional Breakup in Coronet Formation Process; Feb. 1998